Impact of Airfoil Profile on the Supersonic Aerodynamics of Delta Wings

Richard M. Wood* and David S. Miller*
NASA Langley Research Center, Hampton, Virginia

A theoretical study of the effect of airfoil profile on the aerodynamics of delta wings at supersonic speeds has been conducted using a full-potential solution method. Analysis was performed for wings of aspect ratio A of 0.5 to 3.0 over a range of values of the leading-edge sweep-parameter $A\beta$ from 0.5 to 4.0 for diamond, circular arc, and NACA modified 4-digit airfoils. The primary intent of the study was to establish the "real flow" aerodynamics of delta wings for various airfoil shapes. A set of zero-lift wave drag curves for delta wings, which can be used to account for nonlinear aerodynamics in the preliminary design process, has been defined. The predicted zero-lift wave drag differed substantially from the linear theory predictions for all airfoils. The analysis of the modified 4-digit airfoil series showed that the zero-lift wave drag is independent of airfoil leading-edge radius. The linear theory dependence parameter ($C_{D,w}$ varies with thickness τ^2 and aspect ratio A) was verified for thin wings. A detailed study of the surface pressures revealed that for all airfoil geometries analyzed, 90% of the wave drag was produced at the wing apex and trailing edge. The lifting characteristics were also evaluated for the various airfoil profiles, and the results indicated that for β cotΛ values greater than 0.6, the lift-curve slope is less than that predicted by linear theory. Nonlinear analysis also showed that increasing the airfoil bluntness increased the wing's lift-curve slope and decreased its drag-due-to-lift characteristics. For blunt leading-edge airfoils, increasing the airfoil thickness and wing aspect ratio and decreasing the maximum airfoil thickness position reduced the drag-due-to-lift parameter. The drag-due-to-lift characteristics were also found to be sensitive to Mach number and lift coefficient in addition to the known dependence upon aspect ratio and the leading-edge-sweep parameter that is predicted by linear theory.

Nomenclature

A	= wing aspect ratio
$A\beta$	= leading-edge-sweep parameter for zero-lift wave drag
b	= wing span
c	= wing chord
C_D	= drag coefficient
$C_{D,w}$	= zero-lift wave drag coefficient
$C_D(X)$	= sectional drag coefficient $= 1/S_{-YLE}\int^{YLE} C_P(X,Y) - \tan(dZ/dX)(X,Y)\Delta X dY$
ΔC_D	= change in drag coefficient relative to a flat wing at zero lift
$(\Delta C_D/\beta C_L{}^2)$	= drag-due-to-lift parameter
C_L	= lift coefficient
$C_{L,\alpha}$	= lift-curve slope evaluated at zero lift
Cp	= coefficient of pressure
L	= maximum configuration length
m	= position of airfoil maximum thichness expressed as a fraction of the local chord
M	= Mach number
r	= position of airfoil maximum thickness
R	= leading-edge radius parameter for NACA modified 4-digit airfoil series: leading-edge radius $= c[1.1019(\tau R/6)^2]$
S	= wing reference area
$S(X)$	= local wing cross sectional area
t	= wing airfoil thickness
X, Y	= streamwise and spanwise coordinates, respectively
YLE	= spanwise position of leading edge
Z	= vertical coordinate
α	= angle of attack
β	$= \sqrt{M^2-1}$
$\beta C_{L,\alpha}$	= lift-curve-slope parameter
$\beta\cot\Lambda$	= leading-edge-sweep parameter at lifting conditions
τ	= airfoil thickness parameter expressed as a fraction of the local chord
Λ	= wing leading-edge-sweep angle

Subscripts

REF	= reference
C	= crossflow

Presented as Paper 85-4073 at the AIAA 3rd Applied Aerodynamics Conference, Colorado Springs, CO, Oct. 14-16, 1985; received Nov. 4, 1985; revision received March 24, 1986.

*Aero-Space Technologist, Fundamental Aerodynamics Branch, High-Speed Aerodynamics Division. Member AIAA.

Introduction

In the design of an optimum wing at supersonic speeds, the aerodynamics must select from an infinite array of wing planforms, camber and twist distributions, and airfoil profiles. Historically, airfoil profiles have not been emphasized in the wing design cycle. Airfoil profile selection for supersonic flight has been primarily based upon structural considerations and linearized theory aerodynamic estimates. Comparisons of the linear theory estimates with experimental data have shown an inability of the predictions to match experimental results.[1] The lack of an adequate prediction technique has forced the supersonic aircraft designer to take a conservative approach in selecting an airfoil; this has resulted in the use of thin airfoils with sharp leading edges or small amounts of leading-edge bluntness. However, with the recent development of nonlinear flow codes, aerodynamicists can now being to identify and quantify the impact that airfoil profile has on the design of an optimum lifting surface. The available nonlinear flow codes vary in complexity and

capability, and their governing equations range from the inviscid full-potential equation to the Navier Stokes equation. The inviscid full-potential equation should be adequate[2] for the purpose of calculating the impact that changes in airfoil profile have on the aerodynamics of uncambered delta wings at zero, to moderate-lift coefficients.

This paper will present results of a theoretical investigation, in which a series of airfoil profiles are analyzed on delta wings at supersonic speeds. Predicted flowfield, pressure, and force data from the nonlinear full-potential flow code[3] will be presented and compared to both linear theory estimates and experimental data in order to establish design trends and the limitations of linear theory. Results of this study will provide the aerodynamic community with a better understanding of the effect that the airfoil profile can have on the aerodynamics of wings at supersonic speeds and will establish the limitations of linear theory to predict these effects. The results of the theoretical study will be presented in terms of conventional aerodynamic parameters in an effort to consolidate the effects of wing sweep, Mach number, and airfoil shape. In addition, the validity of several linear theory based aerodynamic-wing design rules, which are used daily by the aerodynamicist, will be evaluated.

Discussion

The drag of a body in supersonic flow is predominately composed of both pressure and friction drag. At the zero-lift condition, pressure drag is usually termed wave drag and is due to the volume of the body, while friction drag is due to wall shear stresses. At lifting conditions, an additional pressure drag term develops: the drag due to lift. In general, the present interpretation of drag has never been validated with experimental testing because the interrelation between the drag components cannot be adequately assessed with the existing experimental test techniques. However, through the use of advanced computational methods, inviscid and viscous drag and boundary-layer characteristics can be studied more closely.

This theoretical study is directed at determining the impact of airfoil profile on the aerodynamics of delta wings in an inviscid, supersonic flow. A brief discussion of the geometric and flow parameters under investigation will precede a description of the selected nonlinear-aerodynamic computational method. Theoretical results at the zero-lift condition will then be presented, followed by the predicted lifting characteristics.

Aerodynamic and Geometric Parameters

The identification of an adequate correlation parameter is critical to any parametric study. Linear theory indicates that for delta wings at supersonic speeds all aerodynamic characteristics are a function of the leading-edge flow condition, as described by the leading-edge-sweep parameter ($\beta\cot\Lambda$). The aspect ratio of a delta wing is defined as being four times the cotangent of the wing leading-edge-sweep value (Fig. 1); thus, the leading-edge-sweep parameter also can be expressed in the form of $A\beta$. The present investigation will use the two expressions for the leading-edge-sweep parameters in presenting the results. The $A\beta$ parameter will be used in the discussion of the zero-lift wave drag, and the $\beta\cot\Lambda$ expression will be used in the discussion of the lifting characteristics.

The plots in Fig. 1 represent the range of leading-edge sweep under study and the associated Mach numbers at different points in that range. Wings with aspect ratios varying from 0.5 to 4.0 were selected as representative supersonic planforms (left side of Fig. 1). The variation in Mach number with $A\beta$ is plotted on the right side of Fig. 1. Also indicated in this figure is the sonic leading-edge condition ($A\beta = 4.0$) for delta wings. Nonlinear theoretical analysis will only be presented for values of $A\beta$ less than or equal to 4.0 due to a present limitation in the computational method. The data on the right side of Fig. 1 show that increasing the aspect ratio significantly reduces the Mach number for a given value of $A\beta$.

Theoretical analysis of the effect of airfoil profile on the supersonic aerodynamics of delta wings will include a parametric investigation of the diamond, circular arc, and NACA modified 4-digit airfoil series.[4] Analysis will include the effects of thickness (τ) for all airfoil series; maximum thickness position (m) for the diamond, NACA, and modified 4-digit airfoil series; and leading-edge bluntness (R) for only the NACA modified 4-digit airfoil series. The range of geometric parameters that will be studied are presented graphically in Fig. 2. In this study, thickness will vary from 0.02 to 0.10, thickness position from 0.2 to 0.5, and leading-edge radius parameter from 0.0 to 8.0.

Zero-Lift Wave Drag

Supersonic linear theory suggests that the zero-lift wave drag ($C_{D,W}$) of a delta wing varies as the airfoil thickness-to-chord ratio squared (τ^2) and the wing aspect ratio (A) varies for a given airfoil profile: $C_{D,W} = \tau^2 A f(\beta A, m)$. In 1953, Lawrence[5] incorporated the dependence of the zero-lift wave drag upon Mach number into the standard linear theory drag curves by combining the Mach number, in the form of the parameter β, with the wing geometric parameter A and then plotting the linear-theory-dependence parameter ($C_{D,W}/\tau^2 A$) against the leading-edge-sweep parameter ($A\beta$). This method represents a plot of zero-lift wave drag against Mach number for a given wing geometry, rather than curves showing the effect on wave drag of one or more wing geometric parameters as had been done previously.[6]

The primary intent of this section is to establish the "real flow" dependence of the zero-lift wave drag for delta wings on τ^2, A, and M for various airfoil profiles. Real flow dependence will be established through nonlinear

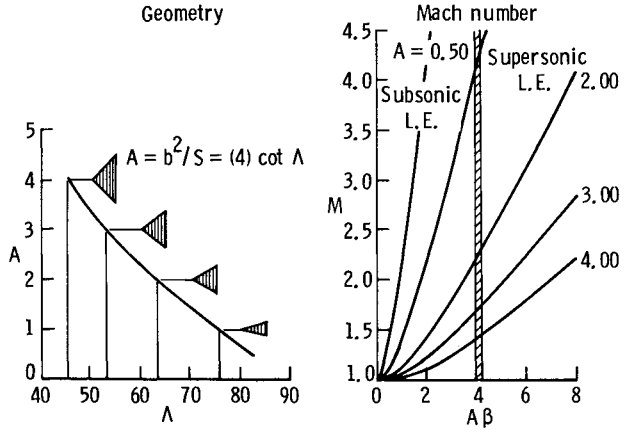

Fig. 1 Aerodynamic correlation parameters.

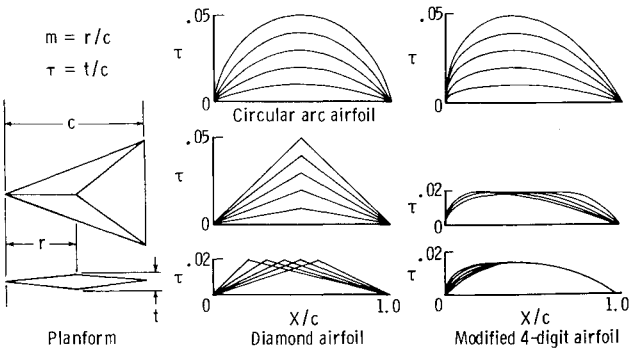

Fig. 2 Geometric parameters under investigation.

aerodynamic analysis with the method of Ref. 3. All zero-lift wave-drag plots will be in the format established by Lawrence.[5]

Diamond Airfoils

The simplicity of the geometry lends itself to a closed-form solution of the linearized equations. A comparison of the nonlinear and linear solutions for delta wings with diamond airfoils is presented in Fig. 3. Nonlinear solutions are obtained with the method of Ref. 3, and the linear solutions are a reproduction of the closed-form solutions presented in Ref. 5. Attempts to duplicate the linear theory solutions with existing thin-wing linear theory computer codes[7] were unsuccessful because of the inaccuracies inherent in the numerical techniques that are employed to solve the equations. Nonlinear and linear theory curves are presented for values of the maximum airfoil thickness position parameter (m) of 0.2, 0.3, 0.4, and 0.5. The nonlinear curves were computed for a 4%-thick delta wing of aspect ratio 1.0. The aspect ratio of 1.0 was selected for nonlinear calculations so that a large variation in Mach number could be analyzed for values of $A\beta$ from 0.5 to 4.0.

Linear theory zero-lift wave drag predictions show a large effect due to airfoil maximum thickness position and increasing $A\beta$. The results indicate that for $A\beta$ values of less than 2.4, a forward shift in the airfoil maximum thickness from 0.5 to 0.2 results in a reduction in drag of 80% and for $A\beta$ values of greater than 3.2, a rearward shift in the airfoil maximum thickness position from 0.2 to 0.5 would also produce a reduction in drag of 80%. For values of $A\beta$ between 2.4 and 3.2, the relationship between the four linear theory curves varies considerably. In this range of $A\beta$, the airfoil maximum thickness lines go supersonic (Mach angle exceeds the maximum thickness line sweep angle) for each airfoil at different values of $A\beta$. When the airfoil maximum thickness line sweep angle goes supersonic, a singularity arises in the linear solution that produces a large drag rise (first peak). The second peak of each linear theory curve corresponds to the drag rise associated with the occurrence of a sonic leading-edge condition; this occurs at an $A\beta$ value of 4.0 for delta wings. As the Mach number is increased beyond the sonic leading-edge condition ($A\beta > 4.0$), linear theory predicts a gradual drag reduction for all diamond airfoils.

Nonlinear zero-lift wave drag estimates for the effect of maximum airfoil thickness position and the leading-edge-sweep parameter are similar to the linear predictions; however, the details of the four nonlinear curves are significantly different. Both linear and nonlinear theory predict a crossover in the four curves, but the linear theory predicted that crossover occurs over a range of $A\beta$ values from 2.4 to 3.2, while the nonlinear theory predicted that crossover for all curves occurs at an $A\beta$ value of 2.4. The nonlinear analysis indicates that at an $A\beta$ value of 2.4, the drag of a delta wing with a diamond airfoil is independent of airfoil maximum thickness position. On either side of this crossover point in the drag curves, the effect of maximum airfoil thickness position is similar to that predicted by linear theory. In general, the nonlinear analysis results show a much smoother variation with $A\beta$ (no peaks or valleys) and lower drag than the linear theory estimates. Nonlinear theory predicts lower drag for most conditions.

The large differences in drag predicted by the linear and nonlinear theories do not solely establish the existence of nonlinear flow, such as large shocks or expansions, over the wings. A major contributor to the large differences predicted by the two methods is that the linear method tends to predict a sharp pressure gradient due to local surface discontinuities, while the nonlinear method predicts a much more gradual change in pressure. For small values of $A\beta$, the flow is subcritical in the crossflow plane ($M_C < 1.0$), and the linear and nonlinear predictions are in close agreement. At large values of $A\beta$ the two solutions are quite different due to both the development of supercritical crossflow conditions ($M_C > 1.0$) and the more accurate modeling of the compressions and expansion fields within the nonlinear code. However, for intermediate values of $A\beta$, the flow about the wing is relatively subcritical, yet the differences between the curves are significant. This is especially true for an $A\beta$ value of 2.4 where the nonlinear method predicts that the drag is independent of airfoil shape. To provide insight into the flow condition at this point, spanwise surface pressure distributions from the nonlinear analysis are shown in Fig. 4 for a 4%-thick delta wing of unit aspect ratio at a Mach number of 2.60 ($A\beta = 2.4$). Predicted pressure results are presented for $m = 0.2$ and 0.5 airfoils at streamwise positions of 20, 40, 60, and 80% of the root chord. A comparison of the pressures for the two airfoils shows a smooth and subcritical character for both, with maximum pressure gradients occurring for the $m = 0.2$ airfoil. The forward movement in the airfoil maximum thickness position creates an effectively blunter airfoil, ($m = 0.2$) than the $m = 0.5$ airfoil, which results in larger compression pressures at the leading-edge and lower expansion pressures as the flow expands around the airfoil ridge line.

The equivalent drag values, which result from an integration of the pressure data, are a result of compensating drag characteristics in the streamwise direction. Over the forward portion of the wing ($0 < X/L < 0.3$) the local drag of the $m = 0.2$ airfoil is greater than the $m = 0.5$ airfoil. Between X/L of 0.3 to 0.7, the drag charcteristics are similar; and over the aft portion of the wing ($0.7 < X/L < 1.0$), the drag of the $m = 0.5$ airfoil is greater due to increased slope at the trailing edge.

Nonlinear analysis has shown that the zero-lift wave drag does vary with squared thickness and aspect ratio in the subcritical range ($A\beta < 2.0$); but for higher values of $A\beta$ (supercritical range), the nonlinear results diverge significantly

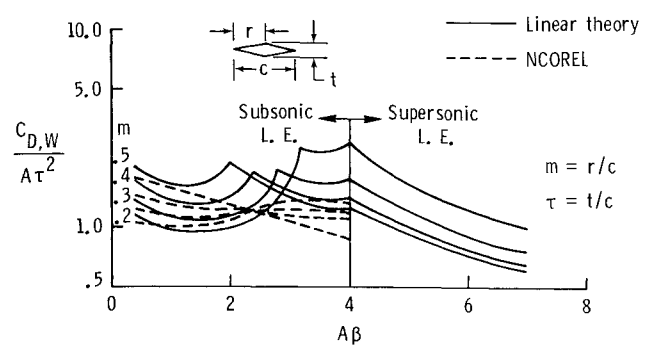

Fig. 3 Linear and nonlinear predicted zero-lift wave drag of delta wings with diamond airfoils.

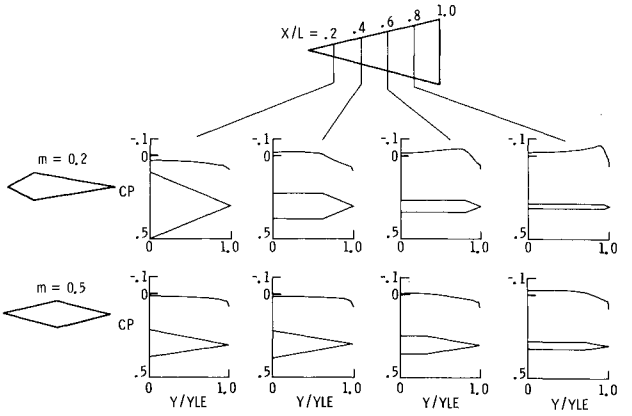

Fig. 4 Nonlinear predicted effect of airfoil maximum thickness position on the spanwise distribution of pressure coefficient for diamond airfoils. $A = 1.0$, $\tau = 0.04$, $A\beta = 2.4$, and $M = 2.60$.

from the linear theory dependence relationship. Within this supercritical range, the nonlinearity of the flow over the wing increases significantly and becomes a strong function of both the wing and airfoil geometry.

Circular Arc Airfoil

The circular arc profile is a unique class of airfoil, which often is used in the design of supersonic vehicles. The circular arc airfoil's uniqueness lies in its single design parameter of airfoil thickness. Compared to the diamond profile, it is probably the most frequent geometry used in fundamental studies of wings. A comparison of the axial distributions of area and drag for a series of equivalent 4%-thick sharp airfoils on a unit aspect ratio delta wing at $M=1.80$ is presented in Fig. 5. The three airfoil profiles are an $m=0.5$ diamond, a circular arc, and a sharp $m=0.5$ modified 4-digit. The diamond airfoil and modified 4-digit airfoil are presented to provide a reference point for discussions on the circular arc profile. The axial distributions of area and drag show that the circular arc airfoil and the equivalent sharp modified 4-digit airfoil ($m=0.5$, $R=0.0$) are very similar; both have greater volume and a different axial drag distribution than the diamond airfoil. The drag characteristics show that the circular arc airfoil has a higher drag at the apex and trailing edge than the diamond airfoil; this is due to the increased surface slopes in these regions.

The effect of $A\beta$ on the nonlinear predicted drag characteristics of the circular arc airfoil is presented in Fig. 6. Also shown in Fig. 6 are the nonlinear drag characteristics of the equivalent modified 4-digit airfoil and the diamond airfoil, along with the linear theory solution for the $m=0.5$ diamond airfoil. Linear theory estimates of the drag characteristics for the circular arc and modified 4-digit geometries are not presented because of the inability of existing thin-wing/slender-body linear theory computer codes to accurately predict the wave drag for the diamond airfoils. Nonlinear analysis shows a smooth variation in drag for values of $A\beta$ between 0.5 and 4.0. Comparison of the drag levels shows that the diamond airfoil has the lowest drag, the modified 4-digit the highest, and the drag of the circular arc profile is just below that of the modified 4-digit profile. These results are consistent with the data presented in Fig. 5.

The results presented in Figs. 5 and 6 indicate that a more complex and nonlinear flow structure exists for the circular arc airfoil than the diamond airfoil. In addition, the characteristics for the circular arc airfoil were shown to be very similar to those for the equivalent modified 4-digit airfoil, suggesting that the circular arc profile can be treated as a subset of the modified 4-digit airfoil family. The analysis shows clearly that the zero-lift drag of equivalent sharp airfoils is not equal. The circular arc has 15 to 40% higher wave drag than the diamond airfoil, but only 4% less drag than the equivalent modified 4-digit airfoil.

Modified 4-Digit Airfoil

The NACA modified 4-digit airfoil series was selected because of the flexibility in defining and altering the airfoil profile. The NACA modified 4-digit airfoil family is defined analytically with the three parameters: airfoil thickness parameter (τ), airfoil maximum thickness position (m), and a leading-edge radius parameter (R). The leading-edge radius of the modified 4-digit series is a function of the a leading-edge radius parameter (R). The leading-edge radius of the modified 4-digit series is a function of the leading-edge radius parameter (R) and the airfoil thickness parameter (τ) only: Leading-edge radius $=c[1.1019(\tau R/6)^2]$. This airfoil family will be used to evaluate the effect of leading-edge bluntness in addition to the effects of τ, m, A, and M on the zero-lift wave drag. Results of the nonlinear analysis for the diamond and circular arc airfoils will be referenced. To provide insight into the geometric character of this class of airfoil, the axial distribution of area and drag for various values of the m and R parameters is presented in Fig. 7. Nonlinear drag characteristics are presented for a 4% thick unit aspect ratio delta wing at $M=1.41(A\beta=1.0)$. The effect of airfoil maximum thickness position is shown at the left of the figure for sharp airfoils. The area distribution shows that moving the airfoil maximum thickness forward results in a forward shift in wing volume and a decrease in the maximum cross-sectional area. These two effects combine to produce a smoother area distribution and lower drag.

A review of the axial distribution of drag for the $m=0.2$ airfoil shows longitudinal symmetry, whereas the drag of the $m=0.5$ airfoil is mostly generated over the final 20% of the wing length. The integrated drag values, which are listed at the top of the figure, show that the $m=0.5$ airfoil has 60% higher drag than the $m=0.2$ airfoil. As Mach number is increased, the character of the drag for each airfoil changes dramatically as the compressive pressures begin to dominate the flow. The apex drag of the $m=0.2$ airfoil would be expected to increase more significantly than the $m=0.5$ airfoil, but the trailing edge drag of both airfoils would decrease.

Shown on the right side of Fig. 7 is the effect of leading-edge bluntness on the axial distribution of area and computed nonlinear drag. Results are presented for a 4%-thick airfoil of $m=0.5$ at R values of 0, 4, and 8, which correspond to a leading-edge radius, expressed as a fraction of the chord, of approximately 0.0, 0.001, and 0.003, respectively. The area and drag data clearly show that leading-edge bluntness only affects the forward half of the wing. Drag data show that increasing airfoil bluntness produces a localized increase in drag at the wing apex followed immediately by a rapid reduction in drag. At an X/L of 0.4, the data show a merging of the drag data for the three airfoils, which then remain coincident over the remainder of the geometry. The crossover in the drag data of the three airfoils, which occurs at the apex of the wing, produces a cancelling effect that results in a drag value of approximately 21 counts (0.0021) for the three airfoils.

The fundamental nonlinear characteristics for the modified 4-digit airfoil series will be established for 4%-

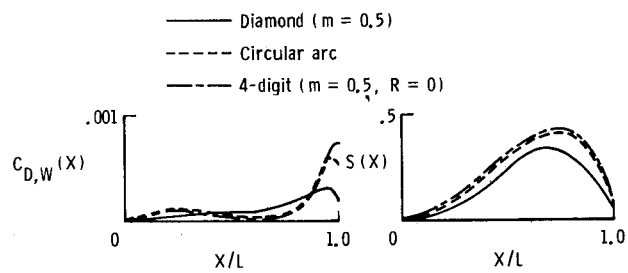

Fig. 5 Axial distribution of wing volume and nonlinear predicted sectional drag for equivalent diamond, circular arc, and sharp NACA modified 4-digit airfoils. $M=1.8$, $A=1$, $A\beta=1.5$, and $\tau=0.04$.

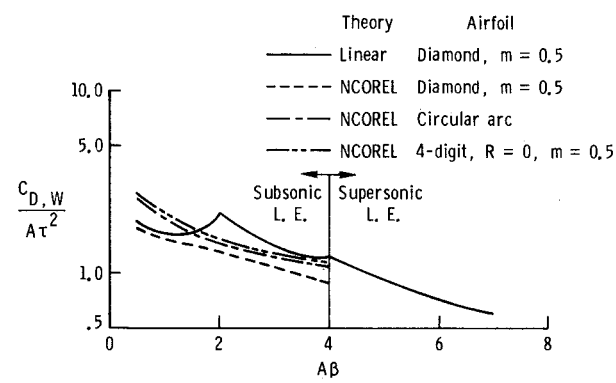

Fig. 6 Predicted nonlinear zero-lift wave drag of delta wings with equivalent diamond, circular arc, and sharp NACA modified 4-digit airfoils.

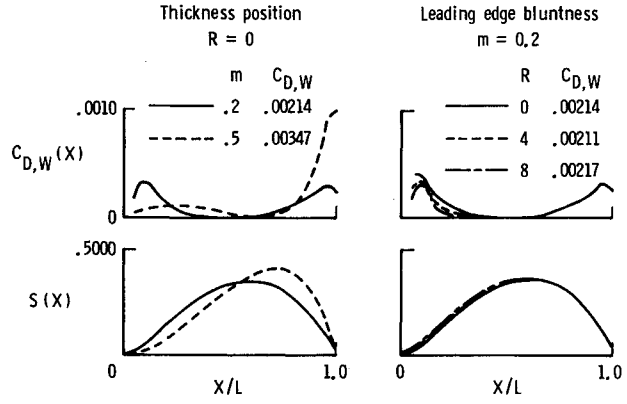

Fig. 7 Axial distribution of wing volume and nonlinear predicted sectional drag for NACA modified 4-digit airfoils. $A = 1.0$, $\tau = 0.04$, and $M = 1.41$.

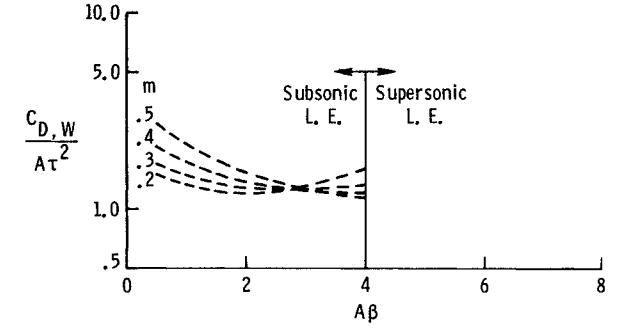

Fig. 8 Predicted nonlinear zero-lift wave drag of delta wings with NACA modified 4-digit airfoils.

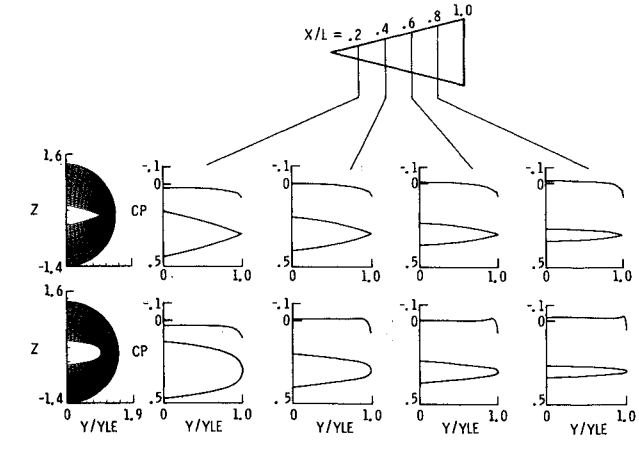

Fig. 9 Nonlinear predicted effect of airfoil leading-edge bluntness on the spanwise distribution of pressure coefficient for NACA modified 4-digit airfoils. $A = 1.0$, $\tau = 0.04$, $M = 0.5$, $A\beta = 3.0$, and $M = 3.16$.

thick, sharp airfoils on an aspect ratio 1.0 wing. The dependence of the drag on the thickness, aspect ratio, and leading-edge bluntness will be established separately.

Presented in Fig. 8 are the nonlinear predicted drag characteristics for sharp modified 4-digit airfoils with maximum thickness locations of 0.2, 0.3, 0.4, and 0.5. Results are presented for $A\beta$ values between 0.5 and 4.0. The nonlinear analysis shows trends similar to those predicted for the diamond airfoil: smooth variations with $A\beta$ and a crossover in the drag of all geometries at a single value of $A\beta$. The crossover in drag for the modified 4-digit series occurs at an $A\beta$ value of approximately 2.8 as compared to a value of 2.4 for the diamond airfoil. The data show that for values of $A\beta$ less than 2.8, moving the maximum airfoil thickness position from 0.5 to 0.2 would reduce the drag by 50%, and for values of $A\beta$ greater than 2.8, a rearward shift in the maximum airfoil thickness position from 0.2 to 0.5 would produce a maximum drag reduction of 30%.

The effect of leading-edge bluntness on the drag characteristics of wings is a highly debatable and important question in the design of wings and complete aircraft configurations. In general, previous supersonic aircraft design studies, which were based upon linear theory, would always employ a sharp airfoil or small amounts of bluntness on the leading edge of the wing in order to minimize the zero-lift wave drag penalty. This design practice has persisted despite recent experimental data[8] that show leading-edge bluntness is not a dominate factor in the zero-lift wave drag of wings.

The nonlinear predicted spanwise surface pressure coefficient data for an aspect ratio 1.0 with 4%-thick, $m = 0.5$ modified 4-digit airfoils of $R = 0.0$ and 8.0 are presented in Fig. 9. The analysis was performed at $M = 3.16$ ($A\beta = 3.0$), which corresponds to geometries that have equivalent drag and are relatively independent of maximum thickness position (see Fig. 8). Predicted pressure distributions are presented for X/L values of 0.2, 0.4, 0.6, and 0.8. The data show that, the blunt airfoil experiences higher surface pressures over the total span at an X/L of 0.2, as compared to the sharp airfoil. For X/L values of 0.4, 0.6, and 0.8, the blunt airfoil experiences an expansion (low pressures) at the leading edge and an overall pressure distribution, which is lower or equal to that of the sharp airfoil. The lower pressures at the leading edge result from the expansion of the flow around the airfoil nose producing an aerodynamic thrust force, which counteracts the drag increase produced by the more positive pressures at the apex of the wing. These findings also support the data presented in Fig. 7 in which the axial distributions of drag for a wing with a sharp and blunt airfoil was shown to cross over just aft of the wing apex, producing a local-drag cancelling effect.

Nonlinear predicted zero-lift drag characteristics of diamond, circular arc, and NACA modified 4-digit airfoils have been shown to vary substantially from the linear theory predicted characteristics. The nonlinear analysis suggests that for slender delta wings at small values of $A\beta$, the linear theory dependence relationship ($C_{D,W}/\tau^2 A$) is maintained. However, as the wing geometry becomes more complex, the flow about the wing becomes more nonlinear, and the linear theory dependence relationship is not maintained. To fully develop the nonlinear zero-lift wave drag curves for delta wings, further analysis would be required. However, the delta wing drag curves presented in Figs. 3, 6, and 8 should be adequate to account for nonlinear effects in the preliminary design process (planform, Mach number, and airfoil selection).

Lifting Characteristics

The ability to take into account the effect of airfoil profile, aspect ratio, and Mach number on the lifting characteristics of delta wings is extremely important in selecting the proper wing geometry. The "real flow" about a delta wing at the zero-lift condition has been shown to be a strong function of these parameters, and as the wing is taken to a lifting condition, the nonlinear effects would be expected to increase significantly. The existing wing design philosophy, which is based upon linear theory, assumes that the lift and drag of a flat wing is only a function of the leading-edge-sweep angle and Mach number. To address this increasingly important problem in preliminary aircraft design, the theoretical nonlinear study of the impact of airfoil profile on delta wings has been extended to include the aerodynamic characteristics at lift. The lifting characteristics will be presented in the form of the lift-curve-slope parameter, and

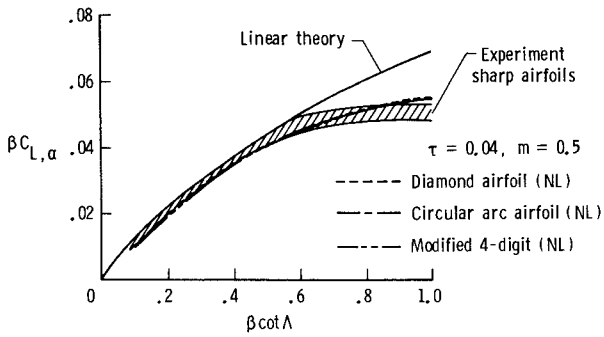

Fig. 10 Comparison of lifting characteristics for equivalent diamond, circular arc, and sharp NACA modified 4-digit airfoils.

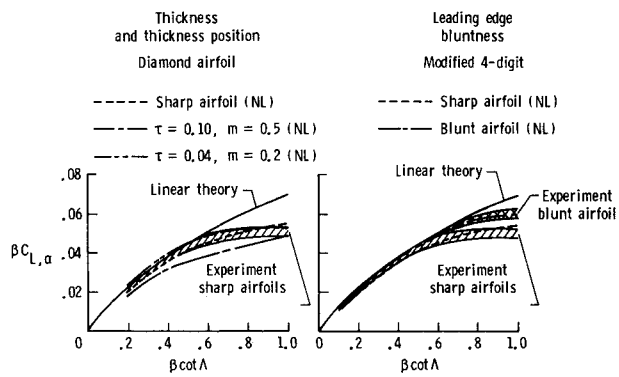

Fig. 11 Nonlinear predicted effect of airfoil thickness, airfoil maximum thickness position, and airfoil leading-edge bluntness on the lifting characteristics. (See Ref. 9.)

the drag will be presented in the form of the drag-due-to-lift parameter.

The nonlinear predicted, linear theory, and experimental data lift-curve-slopes for sharp, thin delta wings with subsonic leading edges are presented in Fig. 10. The data are presented in the form of the lift-curve-slope parameter ($\beta C_{L,\alpha}$) plotted against the leading-edge-sweep parameter ($\beta\cot\Lambda$). Nonlinear analysis is presented for the three equivalent sharp airfoils that were discussed previously. The nonlinear lift-curve slope parameter was computed from analysis at angles of attack of 0 and 1 deg. A comparison of the nonlinear, linear, and experimental results[9] shows that each reduces to a single curve, which is only dependent upon wing leading-edge sweep and Mach number. Figure 10 shows that the nonlinear analysis is in very good agreement with the experimental data and nonlinear analysis for values of $\beta\cot\Lambda$ less than 0.4. For values greater than 0.5, the data and nonlinear analysis show a lower lift-curve-slope than predicted by linear theory. For values of $A\beta$ greater than 2.0, nonlinear analysis at zero lift (Fig. 6) also shows an increase in the nonlinear characteristics. Experimental data and nonlinear analysis show higher pressures than predicted by linear theory for this range of the $\beta\cot\Lambda$. This is especially evident at the leading edge where the linear solution predicts a large negative pressure peak due to the singularity in the solution.

The effect of changes in airfoil thickness, airfoil maximum thickness position, and airfoil bluntness on the lift-curve slope of delta wings is presented in Fig. 11. Presented on the left of Fig. 11 are nonlinear predicted lift-curve slopes for diamond airfoils showing the effect of thickness and maximum thickness position. Also presented in the figure are the linear theory solution and experimental data band. Nonlinear analysis shows that increasing thickness from 4 to 10% significantly reduced the lift-curve slope over the range of analysis. A detailed analysis of this geometry at $\alpha = 1$ deg

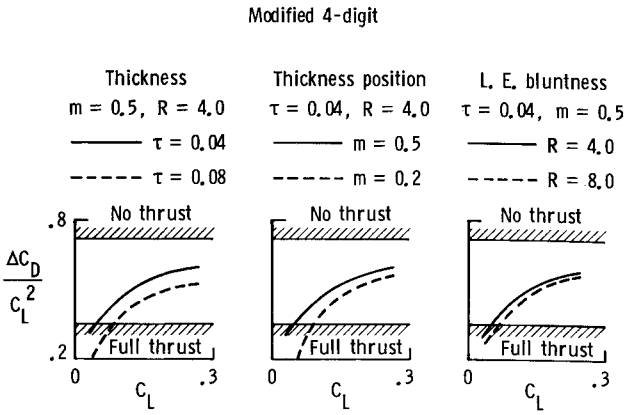

Fig. 12 Nonlinear predicted effect of airfoil thickness, airfoil maximum thickness position, and airfoil leading-edge bluntness on the drag-due-to-lift characteristics. $M = 1.41$, $A = 1.0$, and $A\beta = 1.0$.

revealed the existence of strong nonlinear flow conditions consisting of a supersonic crossflow region at the wing maximum-thickness ridge line and a large positive pressure on the wing upper surface at the leading edge. These results differ substantially from the characteristics that would be predicted by linear theory or those that were predicted by the nonlinear code for the thin-wing geometry.

The effect of moving the airfoil maximum thickness position from 50 to 20%-chord was a slight increase in the lift-curve slope for values of $\beta\cot\Lambda$, less than 0.8, as compared to the $m = 0.5$ airfoil. The data show that the experimental data band for sharp airfoils provides an upper bound, and that the experimental data for thin geometries provides an excellent first approximation of the nonlinear, lifting characteristics. The nonlinear analysis of the characteristics of sharp airfoils could not be extended to larger angles of attack because a leading-edge vortex would form, and the nonlinear full-potential method is only applicable to the attached flow situation.

The effect of airfoil bluntness on the lift characteristics was studied on the modified 4-digit airfoil series. Analysis was performed over a range of angles of attack of 0 to 10 deg in which the linearity of the lift-curve slope was established within 3%. The predicted nonlinear and the experimental data band[9] for blunt airfoils is presented on the right side of Fig. 11. The nonlinear analysis and experimental data are in excellent agreement, and both compare well with linear theory for values of $\beta\cot\Lambda$ less than 0.7. For values of $\beta\cot\Lambda$ greater than 0.7, leading-edge bluntness results in a lift-curve slope below that predicted by linear theory. The data also show that for values of $\beta\cot\Lambda$ above 0.7, leading-edge bluntness will increase the lift-curve slope over that for sharp airfoils. The close agreement between the blunt airfoil data and linear theory is fortuitous; the increased lift-curve slope for the blunt airfoils results from a combination of the increased expansion around the airfoil nose onto the wing upper surface and the increased compression on the lower surface. The flow characteristics described for the blunt airfoil are similar in nature to those that would be predicted by linear theory, but the details of the nonlinear expansions and compressions and the surface on which they act vary significantly from the linear theory model.

Predicted nonlinear drag-due-to-lift characteristics for blunt airfoils are presented in Figs. 12 and 13. The nonlinear method selected for this study can only be applied to the condition of attached flow; as a result nonlinear analysis was limited to blunt airfoils at conditions of low-to-moderate lift coefficients ($C_L \leq 0.3$). The effect of airfoil thickness, airfoil maximum thickness position, and airfoil bluntness on the drag-due-to-lift parameter has been studied on an aspect ratio 1.0 delta wing at a Mach number of 1.41 (Fig. 12). Results of the analysis show that increasing thickness, mov-

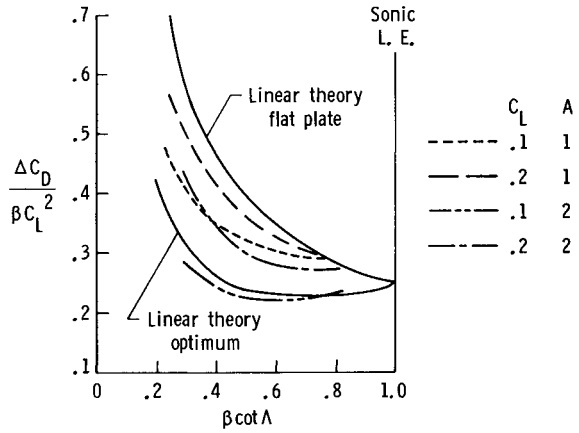

Fig. 13 Predicted nonlinear drag-due-to-lift characteristics for blunt airfoils.

ing the maximum thickness forward, or increasing airfoil bluntness improves the wings lifting efficiency, with airfoil thickness providing the largest improvement and bluntness the smallest. Comparisons of the results show that the nonlinear method predicts a lower drag-due-to-lift parameter than the linear theory for uncambered wings (no thrust), and for low values of the lift coefficient ($C_L < 0.1$), the nonlinear theory predicts drag characteristics below the linear theory optimum (full thrust). The increase in the drag-due-to-lift parameter with increasing lift coefficient is a result of a loss in the aerodynamic thrust as the wing rotates through a range of angles of attack. At low-lift conditions, the flow about the wing surface is characterized by a gradual expansion about the nose of the airfoil followed by a smooth recompression. This combination produces a leading-edge suction force and a large amount of aerodynamic thrust force. As angle of attack is increased to attain a higher lift coefficient, the local expansion about the airfoil nose increases significantly and extends over a greater portion of the wing leeside surface resulting in a smaller percentage of the local expansion pressures acting on the nose of the wing. This results in a reduction in the wing's aerodynamic thrust force. The favorable flow conditions that exist about the nose of a blunt airfoil (low pressures) must coincide with favorable flow conditions over the aft section of the airfoil (high pressures) if an improvement in the drag-due-to-lift characteristics is to be realized.

Another observation of the nonlinear analysis that is verified with experimental data is that the drag-due-to-lift characteristics of thick wings with sharp airfoils are similar to those presented for blunt airfoils.[8] The nonlinear analysis of sharp airfoils at low angles of attack shows a quicker rise in the drag-due-to-lift parameter with increasing lift coefficient than was predicted for blunt airfoils. However, the experimental data for sharp airfoils did show a variation from a full thrust to a no-thrust condition between $C_L \approx 0.05$ to $C_L \approx 0.4$, respectively. Only for geometries that approximate a zero thick sharp airfoil did the experimental data show a constant drag-due-to-lift parameter with varying lift coefficient.

Nonlinear analysis has shown that significant amounts of aerodynamic thrust are generated on any thick airfoil profile. The analysis showed an increase in performance for blunt airfoils, as compared to the sharp airfoils; and the performance improvements were maintained over a greater range of lift coefficients.

The nonlinear analysis presented in Fig. 12 was performed at conditions that were previously determined to have a subcritical type flow structure at zero lift ($A\beta = 1.0$ or $\beta\cot\Lambda = 0.25$); however, the drag-due-to-lift analysis showed highly nonlinear characteristics. To investigate these effects further, nonlinear analysis was performed on both an aspect ratio 1 delta wing and an aspect ratio 2 delta wing with blunt, modified 4-digit airfoils ($\tau = 0.4$, $m = 0.5$, $R = 4.0$). Analysis was conducted for values of $\beta\cot\Lambda$ from 0.25 to 0.8. Results of this analysis are presented in Fig. 13, in which curves of constant lift coefficient for both wings are shown. The linear theory flat plate and linear theory optimum curves of the drag-due-to-lift parameter are also presented in the figure. The nonlinear analysis shows an increase in the drag-due-to-lift parameter with increasing lift coefficient, decreasing $\beta\cot\Lambda$, and decreasing aspect ratio. Results for the $A = 1.0$ wing at $C_L = 0.1$ show a variation in the aerodynamic thrust from 70% of the optimum linear theory value at a $\beta\cot\Lambda$ value of 0.25 to 0% at a $\beta\cot\Lambda$ value of 0.75 as compared to the $A = 2.0$ wing at $C_L = 0.1$, where the performance varied from 114 to 100% going from a $\beta\cot\Lambda$ value of 0.25 to 0.75. Similar characteristics also were observed for the two wings at a lift coefficient of 0.2.

The reduced performance with decreasing wing aspect ratio would be expected for a constant Mach number; however, this method of presentation is an attempt to factor aspect ratio effects out of the solution. The analysis suggests that Mach number has a large impact on the aerodynamic performance of a given wing. As the Mach number is reduced, the characteristics of the wing change dramatically; the upper-surface leading-edge suction pressures become more negative and the lower-surface leading-edge pressure reduce considerably, increasing the aerodynamic thrust force. In addition, the thrust force, which is produced normal to the wing leading edge, varies in the streamwise direction as the cosine of the leading-edge-sweep angle. As aspect ratio is increased, the wing sweep will decrease, increasing the aerodynamic thrust force.

In general, the character of all the curves presented in Fig. 13 is a rapid reduction in the drag-due-to-lift parameter (increased performance) with increasing $\beta\cot\Lambda$ up to a value of approximately 0.6. For $\beta\cot\Lambda$ values greater than 0.6 the curves tend to flatten out. This characteristic is seen to be quite sensitive to aspect ratio and lift coefficient; however, a $\beta\cot\Lambda$ value of 0.6 seems to be a representative mean value for the analysis conducted.

Conclusion

A theoretical study of the effect of airfoil profile on the nonlinear aerodynamics of delta wings at supersonic speeds has been conducted. Analysis was performed for wings of aspect ratio 0.5 to 3.0 over a range of values of the leading-edge-sweep parameter $A\beta$ of 0.5 to 4.0 for diamond, circular arc, and NACA modified 4-digit airfoils. The primary intent of the study was to establish the "real flow" aerodynamics of delta wings for various airfoil shapes and, in the process, to evaluate or validate the linear-theory-dependence parameter ($C_{D,W}/\tau^2 A$) for the effect of airfoil shape, wing aspect ratio, and Mach number.

A set of nonlinear zero-lift wave drag curves for delta wings are defined, which can be used to account for nonlinear aerodynamics in the preliminary design process. The nonlinear predicted zero-lift wave drag differed substantially from the linear theory predictions for all airfoils. The data showed that the drag of diamond airfoil at an $A\beta$ value of 2.4 is independent of maximum thickness position. The analysis showed a similar condition occurred for the modified 4-digit airfoil series at an $A\beta$ value of 2.8. The analysis of the modified 4-digit airfoil series also showed that the zero-lift wave drag is independent of airfoil leading-edge radius. The linear-theory dependence parameter ($C_{D,w}$ varies with τ^2 and A) was verified for thin wings, and the analysis indicated the need for a more detailed study to fully resolve the wave drag of wings with large thickness ($\tau \approx 0.10$). A detailed study of the surface pressures revealed that, for all geometries analyzed, 90% of the wave drag was produced at the wing apex and trailing edge.

The lifting characteristics were also evaluated for the various airfoil profiles, and the results indicated that for values of $\beta\cot\Lambda$ greater than 0.6 the nonlinear lift-curve slope is less than predicted by linear theory. Nonlinear analysis also showed that increasing the airfoil bluntness increased the wing's lift-curve slope and decreased drag-due-to-lift characteristics. For blunt leading-edge airfoils, increasing airfoil thickness, increasing wing aspect ratio, and decreasing the maximum airfoil position reduced the drag-due-to-lift parameter. The drag-due-to-lift characteristics also were found to be sensitive to Mach number and lift coefficient in addition to the known dependence upon aspect ratio and $\beta\cot\Lambda$ that is prediced by linear theory.

As the flow becomes more nonlinear, additional concerns arise beyond grid resolution, such as the accuracy of the force integration routines, boundary layer effects, and possible flow separation. All of these effects need to be accounted for in future analysis. However, the results presented in this paper should be representative of the "real flow" aerodynamic characteristics of delta wings.

References

[1]Weber, J. and King, C., "Analysis of the Zero-Lift Wave Drag Measured on Delta Wings," R&M No. 3818, British A.R.C., 1978.

[2]Mason, W.H., "A Wing Concept for Supersonic Maneuvering," NASA CR-3763, Dec. 1983.

[3]Siclari, M.J., "The NCOREL Computer Program for 3D Nonlinear Supersonic Potential Flow Computations," NASA CR-3694, Aug. 1983.

[4]Abbott, I.H. and Doenhoff, A.E., *Theory of Wing Sections,* Dover Publications, 1959.

[5]Lawrence T., "Charts of the Wave Drag at Wings at Zero Lift," C.P. No. 116, British A.R.C., 1953.

[6]Puckett, A.E., "Supersonic Wave Drag of Thin Airfoils," *Journal of Aeronautical Science,* Vol. 13, No. 9, 1946.

[7]Middleton, W.D., Lundry, J.L., and Coleman, R.G., "A System for Aerodynamic Design and Analysis of Supersonic Aircraft," *Part 2-User's Manual,* NASA CR-3362, 1980.

[8]Wood, R.M. and Miller, D.S., "Experimental Investigation of Leading-Edge Thrust at Supersonic Speeds," NASA TP-2204, 1983.

[9]Wood, R.M. and Miller D.S., "Assessment of Preliminary Prediction Techniques for Wing Leading-Edge Vortex Flows at Supersonic Speeds," AIAA Paper 84-2208, Aug. 1984.